Progress in Organic Coatings 197 (2024) 108827

Contents lists available at ScienceDirect

Progress in Organic Coatings

journal homepage: www.elsevier.com/locate/porgcoat

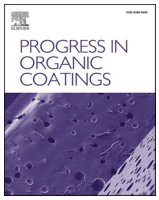

Antiviral respiratory masks with plasma-functionalized polypropylene textiles for optimal adsorption of antiviral substance

Mark Zver [a,b], David Dobnik [c], Rok Zaplotnik [a], Miran Mozetič [a], Alenka Vesel [a], Arijana Filipić [c], Polona Kogovšek [c], Katja Fric [c], Alja Štern [c], Gregor Primc [a,*]

[a] Department of Surface Engineering, Jozef Stefan Institute, Jamova cesta 39, 1000 Ljubljana, Slovenia
[b] Jozef Stefan post-graduate school, Jamova cesta 39, 1000 Ljubljana, Slovenia
[c] National Institute of Biology, Večna pot 111, 1000 Ljubljana, Slovenia

ARTICLE INFO

Keywords:
Surgical face masks
Plasma functionalization
Antiviral materials
Virus filtration
Breathability
Cytotoxicity

ABSTRACT

During the COVID-19 pandemic, face masks were the first line of defense against the spread of infection. However, infectious viruses may remain on medical textiles, potentially serving as an additional source of infection. Due to their chemical inertness, many textiles cannot be enhanced with antiviral functionalities. Through treatment with low-pressure gaseous plasma, we have activated the surface of a medical-grade melt-blown, non-woven polypropylene textile so that it can absorb sodium dodecyl sulfate, an antimicrobial surfactant. Within two hours of contact time, the functionalized textile has been able to inactivate over 7 $\log_{10}$ PFU mL^{-1} of bacteriophage phi6, a surrogate of enveloped viruses such as SARS-CoV-2, and it has retained its antiviral properties for over 100 days. The functionalized material has not disrupted facial mask filtration efficiency or breathability. In addition, the in vitro biocompatibility testing in accordance with ISO 10993-5 for testing of medical devices has demonstrated that the selected formulation causes no adverse effects on the mouse fibroblast cell line L-929. With the treatment processes that have been completed within seconds, the method seems to have great potential to produce antiviral textiles against future outbreaks.

1. Introduction

On March 11th 2020, the World Health Organization (WHO) officially declared the COVID-19 pandemic due to concern about the spread and severity of the disease. SARS-CoV-2 was thought to be primarily transmitted from an infected person via aerosolized droplets, which prompted all nations globally to implement strict mask-wearing. Face masks of various grades have been shown to be able to limit the spread of pathogen-containing droplets [1]. Medical face masks are low cost and, when worn correctly, prevent at least 95 % (surgical face mask, type I) of droplets with an average size of >0.3 μm from reaching their opposite side [1]. They do so by either reflecting incoming water droplets or capturing them, thus preventing them from coming into contact with the wearer [2]. While such masks may be inconvenient for everyday use, they are currently the best solution our society has to limit airborne transmission of pathogens. The filtering of viral particles may be pretty efficient, but some viruses, including SARS-CoV-2, remain viable on personal protective equipment (PPE) for several days and could present an additional source of infection through prolonged use [2]. Indeed, the transmission by touching an infected mask and then eyes, mouth, or nose could directly transfer viral particles in close proximity to their respective host cells. The tendency of viruses to remain viable on surfaces and textiles has inspired much research aimed at developing antimicrobial surfaces. Non-woven polypropylene (PP) is one of the most common materials for producing medical masks and PPE. During the melt-blowing process, this thermoplast is melted and spun into filaments randomly distributed in non-woven textiles, demonstrating good filtering properties. Polypropylene has many desired properties for constructing facial masks. It has one of the lowest densities of any polymer while not lacking in mechanical strength and durability. Polypropylene has been the substrate of choice for many antimicrobial surface applications due to its low cost and broad utility, but the ability to inactivate pathogens would be a definite improvement.

The primary approach to producing an antimicrobial textile is to functionalize it to effectively inactivate the targeted microorganisms (e.g., coating it with antimicrobial agents). These coatings can either

* Corresponding author.
E-mail address: gregor.primc@ijs.si (G. Primc).

https://doi.org/10.1016/j.porgcoat.2024.108827
Received 14 June 2024; Received in revised form 30 August 2024; Accepted 20 September 2024
Available online 25 September 2024

continuously release the antimicrobial substance or inactivate pathogens upon contact [3,4]. Another approach is to produce textiles that repel pathogens [5]. Such textiles do not inactivate the pathogens but prevent them from remaining on the textile and causing further infections (Fig. 1). Reviews on various approaches to the synthesis of such materials and how they interact with microbes have been published [5–7].

Previously, antimicrobial PP has been prepared through functionalization with various compounds such as rose Bengal [8], chitosan [9,10], metal nanoparticles [11], N-halamines [12], quaternary benzophenone-based coatings [13], enzymes [14], and plant extracts [15,16]. Besides research approaches to develop new antimicrobial PPE, companies already have their antiviral masks on the market, containing metal oxides (e.g., Cupron – Cu_xO, Nexera – AgCu, Sonovia – ZnO) and other compounds (e.g., GSK – citric acid) with known biocidal action, demonstrating the maturity and readiness of the market to uptake such technologies [17]. Other advanced alternatives have been tested on non-polypropylene materials, such as non-woven polyamide 6 functionalized with negatively charged linear polyglycerol sulfate as a virus-binding functional group [18], covalently immobilized chlorine membranes made of polyurethane [19], TiO_2 nanowires on filter paper [20], or antibacterial nanofibers prepared by a solution electrospinning method with hydrogen-bonded organic frameworks and poly(vinylidene fluoride-co-hexafluoro-propylene) [21].

Other approaches include coating with dermatologically approved biofunctional solidified commercial hand soap at the concentration of about 0.6 *w*/w %, as reported by Vicent et al. [22]. This treatment enabled 100 % inactivation of selected viruses within a minute after deposition. Takayama et al. [23] impregnated the non-woven filter textiles with two types of cranberry extracts and reported over 3 log reduction of SARS-CoV-2 after 1 min of contact as compared to untreated textiles. Maton et al. [24] functionalized polypropylene filters with a cyclodextrin (CD)-polycarboxylic acid-crosslinked polymer (PP-CD) through a pad/dry/curing process. The materials were then activated by padding in an alkyl dimethyl benzalkonium chloride (ADBAC) solution. The virucidal effect was probed with human coronavirus HCoV-229E, and the 3-log reduction was reported about 10 min after deposition.

Polypropylene is chemically resistant and exhibits low surface energy, which is ideal for repelling incoming droplets potentially containing pathogens. On the other hand, its hydrophobic nature makes it difficult to modify through additional treatment. PP needs to be pre-treated to increase its surface-free energy, overcome its chemical inertness, and make it better suited for dyeing, bonding, wetting, etc. This can be achieved by applying an oxidizing flame, chemical oxidation (e.g., chromosulfuric acid), or an electrical discharge, i.e., plasma treatment [25]. Every method has its advantages and shortcomings, but when rapid, efficient, and sustainable treatment of textiles is needed, low-temperature (cold) plasma is preferred [26]. Plasma can be used as a technology to prepare surfaces with active (antimicrobial) coating, repelling coating, or nanostructured morphology (Fig. 1). Besides tailoring surface properties, gaseous plasma can be used as a sterilization technology to actively inactivate microbes on textile materials (Fig. 2).

Plasma is an ionized gas, usually sustained by an electric field.

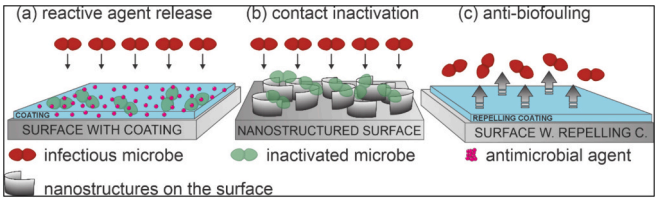

Fig. 1. Methods to inactivate microbes on textile materials using plasma as a technology for surface pre-treatment to coat a surface with an antimicrobial agent (a), nanostructure a surface (b), or prepare a repelling coating.

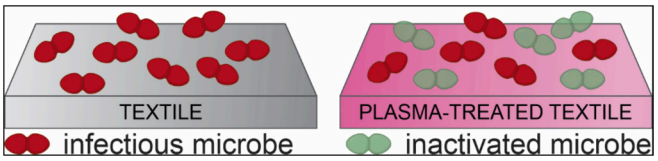

Fig. 2. Using plasma as an active technology for disinfection/sterilization.

Besides free electrons and ions, it contains many other reactive species like neutral atoms, metastable molecules, and photons. Plasma species react with the surfaces of materials, causing their modification, so plasma treatment is an ideal technique for tailoring the surface properties of materials. Selecting appropriate discharge parameters and experimental configuration makes treating the materials at room temperature and under controlled conditions possible. Low-pressure plasmas can be generated in large volumes and are suitable for large-scale industrial applications. Required treatment times can be very short in the order of seconds. Low-pressure plasma requires a vacuum system, but otherwise, the treatment costs can be low enough to make it the ideal method to improve the wettability of hydrophobic materials. An alternative to low-pressure plasmas is atmospheric-pressure plasmas sustained by corona or dielectric barrier discharges. However, the filamentary character of such discharges can cause less uniform surface treatment on the microscopic scale. Plasma techniques suitable for making polymers antiviral were reviewed by Ma et al. [27]. Cold plasma has been previously used to enhance PP for improved cesium absorption [28], antimicrobial activity [14,29–31], dye removal [32], membrane separation [33,34], and improved hemocompatibility [35].

With improved textile wettability, polar solutions of known antimicrobial compounds can be effectively applied to medical-grade materials at sufficient concentrations to inactivate viruses while being entirely safe for the wearer. One such compound is sodium dodecyl sulphate (SDS), an anionic surfactant present in everyday household products ranging from detergents to cosmetics [36]. It consists of a polar sulphate group and a nonpolar hydrocarbon tail and exhibits microbiocidal properties by disrupting the lipid envelope or causing protein denaturation, which may result in virus inactivation. [37,38]. Its cytotoxicity is not definitively known; however, it is presumed safe in concentrations below 1 % [39]. In this work, we used low-pressure gaseous plasma to improve the wettability of the PP outer layer of medical masks and impart antiviral properties to them using SDS. Antiviral activity was evaluated in accordance with the ISO 18184:2019 standard [40] using bacteriophage phi6 as a surrogate of enveloped viruses such as SARS-CoV-2 [41] and aging was assessed. We have also characterized the material following international standards in terms of cytotoxicity (ISO 10993-5:2009, [42]), breathability, and viral filtration (EN 14683:2019 + AC:2019, [43]).

2. Materials and methods

2.1. Preparation of antiviral polypropylene textiles

Medical-grade melt-blown, non-woven polypropylene (PP) and melt-blown polyethylene terephthalate (PET) fabric, which are used to construct commercial masks, were obtained from the company Omega Air (Omega Air d.o.o., Ljubljana, Slovenia). The PP layer serves as the outer and inner layer, while PET is the filtering middle layer, which was only used for the mask construction and was not further modified. Disinfected scissors were used to cut squares from the fabric roll to prepare smaller samples of PP for further treatment. For studying antiviral activity, aging, and inactivation kinetics, PP samples were cut into 2 cm × 5 cm pieces and were treated in a small vacuum system where the plasma was sustained by an inductively coupled radiofrequency (RF) discharge (details of the plasma systems are presented below). For breathability, filtration efficiency, and mask antiviral activity, the PP

samples were cut into 10 cm × 10 cm size and treated in a larger system with almost identical fluence of neutral oxygen atoms. The 10 cm × 10 cm samples were further cut into 3 cm^2 pieces for the biocompatibility test. Three-layered medical masks were constructed for viral filtration and breathability tests by joining the two PP layers (outer and inner) with PET (middle) from the same manufacturer. To prepare the antiviral PP layer, PP was functionalized with SDS after plasma treatment.

A 100 mM stock solution of SDS (Sigma-Aldrich, USA) was prepared with MilliQ water, sterilized by filtration (0.2 μm pore size), and pH adjusted to 7.2. After the plasma treatment of PP, three different SDS dilutions were applied to the sample. The dilutions were 1 %, 0.25 %, 0.1 %, and 0.05 % (*w*/w %), which denotes the weight of applied SDS per weight of material expressed as a percentage (e.g., 10 μg of SDS per 1 mg of PP is 1 % SDS). The desired amount of SDS was applied in a 2 μL volume per mg of material by distributing it evenly on the cut material with a pipette and left to dry at room temperature for 1 h. The control received the same volume of MilliQ water. Several additional samples were prepared and individually placed in Eppendorf tubes to be stored in the dark at room temperature and later used to evaluate the textile's antiviral durability (i.e., aging).

2.2. Small plasma device

Plasma treatment of materials for studying viral inactivation was performed in a radiofrequency inductively coupled plasma (RF ICP), shown in Fig. 3.

The system comprises a borosilicate glass discharge tube (inner diameter of 36 mm and length of 750 mm) evacuated with an Edwards E2M80 (Edwards, USA) two-stage pump. A 2 cm × 5 cm material was placed in the middle of the RF plasma coil (glow region), and the system was evacuated via a vacuum pump down to a base pressure of 1 Pa (0 sccm O_2). Plasma was ignited in either base pressure (predominantly water vapor) of ~1 Pa or was supplied with 5 sccm or 30 sccm of O_2 to a final pressure of 4.5 Pa and 12.9 Pa, respectively. The material was treated in *E*-mode plasma sustained at an applied power (W_{real}) of 10 W or 13 kW/m^3 of plasma. The small plasma device had a glowing plasma volume of approximately 0.00075 m^3. The treatment time varied between 1 and 10 s. The discharge is sustained with a Cesar 1310 RF generator (Advanced Energy, USA) operating at 13.56 MHz, connected to a water-cooled 6-loop copper coil and an Advanced Energy Vari-oMatch (Advanced Energy, USA) impedance matching network. Gas flow was adjusted with the Aera FC-7700 (Advanced Energy, USA) mass flow controller, and the pressure was measured with an absolute capacitive pressure gauge (MKS Baratron, Type 722A, USA). The power applied to the system is consistently cited as the difference between the input or forward and reflected power, denoted as W_{real}. After plasma treatment, the textile samples were exposed to air at ambient conditions, and appropriate SDS concentrations were applied. After drying at ambient conditions for 2 h, a hole-punch was used to cut small circles of material (5 mm diameter, 1 mg weight), which were placed in either a 96-well microtiter plate (Corning Costar, ultra-low attachment surface 3474) for antiviral activity experiments or individually placed in Eppendorf tubes to be stored in the dark at room temperature for later use to evaluate the textile's antiviral durability, i.e., aging.

2.3. Large plasma device

Larger PP pieces (10 cm × 10 cm) of PP were treated in an industrial-size plasma system with a borosilicate glass discharge tube measuring 200 cm in length and 19 cm in inner diameter. The material was placed in the middle of the copper coil surrounding the glass tube and evacuated to a base pressure of ~1 Pa (0 sccm O_2) with a two-stage rotary pump Leybold Trivac D65B, with a nominal pumping speed of 65 m^3 h^{-1}. Oxygen was supplied in the tube with Area FC7700 mass flow controller (Advanced Energy, USA) to reach 15 Pa, after which the plasma was ignited. The plasma was generated by a five-turn bifilar excitation coil connected to a 27.12 MHz RF generator (UHFG-8, Induktio, Slovenia) through an L-type impedance matching network, using the real power of 1.7 kW and the plasma treatment time of 1 s enabled optimal wettability of the PP samples. The 1-s treatment provided approximately the same fluence of neutral oxygen atoms as the 10-s treatment in the small plasma reactor (see Table 1). After the plasma treatment, the sample was exposed to air at ambient conditions, and 2 μL of appropriate SDS dilution per mg of material was pipetted evenly on the material and left to dry at room temperature for 3 h. Subsequently, we could proceed with the experiments (e.g., VFE, virus inactivation on masks, breathability, and biocompatibility).

2.4. Measurements of neutral oxygen atoms and small/large plasma system comparison

As already stated, several characterization methods require larger samples, which had to be prepared in a bigger plasma setup. To provide adequately plasma-treated surfaces when moving from the smaller to the bigger reactor, we measured the density, flux, and fluence of neutral oxygen atoms (Table 1), the main acting plasma particles in our plasma reactor configurations and gas. We used catalytic probe measurements to determine the density of neutral oxygen atoms in both reactors [44]. Briefly, the probe acts as a precise temperature-sensing device with a

Table 1
O-atom density (n_O), flux, and fluence applied to the textile material in two different plasma systems.

Plasma device	Small plasma system	Large plasma system
Pressure (Pa)	4.5	15
Applied power density (kW m^{-3})	13	30
n_O (× 10^{20} m^{-3})	1.7 ± 0.25	15 ± 2.5
O-atom flux (× 10^{22} m^{-2} s^{-1})	2.6 ± 0.4	23 ± 3
O-atom fluence (× 10^{23} m^{-2})	2.6 ± 0.4	2.3 ± 0.3

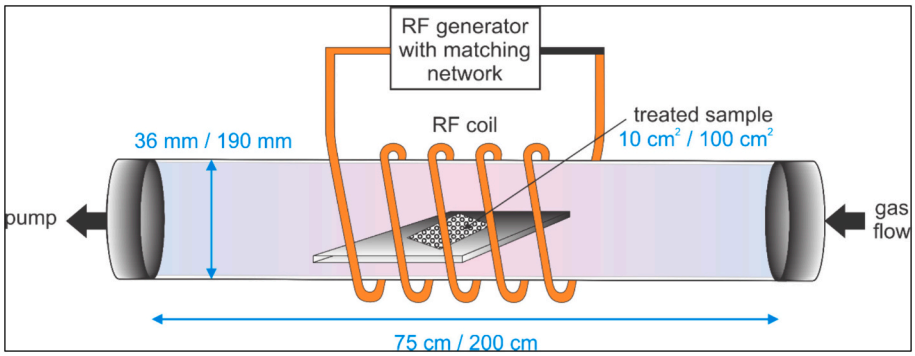

Fig. 3. Schematic representation of textile treatment with 'small' (dimensions on the left) and 'large' (dimensions on the right) RF plasma device.

round tip made of a catalytic material (metal oxide for neutral oxygen atoms) that promotes an exothermic reaction of neutral oxygen recombining with oxygen molecules, leaving the probe's surface. These reactions heat the probe tip, making it possible to determine the influx of the recombined plasma particles. Ions have a minimal effect on heating because plasma is weakly ionized and has low power. More about the catalytic probes and their use is described elsewhere [44,45]. Cobalt was used as the catalytic material for these particular measurements. The probe tip was a round disc of 3 mm in diameter and 50 μm thick and was activated prior to measurements, i.e., oxidized in oxygen plasma so that a stable oxide film was formed on the tip's catalytic surface. The flux and fluence of the best treatment in the small plasma setup at 4.5 Pa total pressure and 5 sccm of oxygen were used as a reference to tweak similar flux and fluence in the big plasma setup. As evident from Table 1, the density and flux of neutral oxygen atoms in the big plasma setup were roughly an order of magnitude larger compared to the small plasma setup. That is why the treatment times were adjusted and were 10 times shorter in order to treat larger samples with the same fluence as the smaller samples: 2.6×10^{23} neutral oxygen atoms/m^{-2} in the smaller reactor in 10 s versus 2.3×10^{23} oxygen neutral atoms/m^{-2} in the large reactor in 1 s. The measurements confirmed that both samples were similarly treated from the plasma point of view, which was also evident by the efficient absorption of the SDS solution in the treated material.

2.5. Surface analysis

The wettability of PP samples treated in the small plasma setup was evaluated by depositing a small water droplet and measuring the water contact angle (WCA) with the Drop Shape Analyser DSA 100E (Krüss GmbH, Germany). A static contact angle was measured using a sessile drop method and MilliQ water. Within a minute after plasma treatment, a 2 μL MilliQ water droplet was deposited on the material, with at least three droplets per sample deposited at different locations. The WCA was measured 10 s after its deposition, and an evaluation was performed in triplicates.

Modification of the surface composition of PP textiles before and after plasma treatment in the small system was investigated by X-ray photoelectron spectroscopy (XPS). Samples were characterized by an instrument model called TFA XPS (Physical Electronics, Munich, Germany). The samples were irradiated with monochromatic Al $K\alpha_{1,2}$ radiation with a photon energy of 1486.6 eV. The diameter of an analysis area was approximately 400 μm. Photoelectron spectra were measured at an electron take-off angle of 45°. Survey spectra were measured at a pass energy of 187 eV using an energy step of 0.4 eV, whereas high-resolution C1s spectra were measured at a pass energy of 29.35 eV using an energy step of 0.125 eV. Because the samples are insulators, an additional electron gun was used to compensate for the accumulated surface charge during irradiation with X-rays. Measured spectra were analyzed using MultiPak v8.1c software supplied with the spectrometer. Shirley-type background subtraction was applied. High-resolution spectra were fitted with Gauss-Lorentzian functions.

2.6. Viral inactivation on PP and aging

Determination of virus inactivation of functionalized PP samples (i.e., treated with the small plasma device) was done by adhering to the ISO 18194:2019-Determination of antiviral activity of textile products guidelines [40] and implementing the spot-titer culture assay methodology described by Beck et al. [46]. A 2 μL of viral stock solution (working concentration ~ 10^7 PFU mL^{-1}) was placed on the small textile circles (diameter of 5 mm) and incubated for 2 h, as per the ISO standard. Following the 2-h incubation period, 200 μL of SM buffer was added to the sample, and a 1:4 serial dilution was performed with 50 μL sample being added to 150 μL of SM buffer repeatedly. To evaluate the binding of viruses to the treated material, the viral samples were also placed on plasma pre-treated samples, with the SDS solution exchanged for MilliQ water. Virus inactivation was determined as described below (section Infectivity assays). All measurements were performed in triplicates.

The treatment's durability was performed weekly using treated materials stored at room temperature to evaluate if functionalized PP retains its antiviral activity in time (i.e., aging). Additionally, the time-dependent inactivation of viruses was examined by exposing the virus to treated material with the lowest (0.1 *w*/w %) SDS concentration for 0.5, 1, or 2 h and quantifying the amount of inactivated virus, as explained above.

2.7. Infectivity assays

All antiviral assays (virus inactivation on PP and masks) were performed using bacteriophage phi6 (DSM 21518) and its host bacteria *Pseudomonas syringae* van Hall 1902 (DSM21482). For determination of virus inactivation, 200 μL of overnight *P. syringae* bacterial culture, grown in liquid TSB (30 g L^{-1} TSB, 1.93 g L^{-1} $MgCl_2$) was used to inoculate 5 mL of liquid 'top agar'(30 g L^{-1} TSB, 7 g L^{-1} agar, 1.93 g L^{-1} $MgCl_2$), mixed and poured over the agar plates (30 g L^{-1} TSB, 15 g L^{-1} agar, 1.93 g L^{-1} $MgCl_2$), and left to solidify. These plates were then inoculated with 4–5 drops of 10 μL volume of virus sample dilutions and incubated at 25 °C overnight. The following day, the plaques were counted, and virus concentration/inactivation was calculated as follows: *Inactivation* ($\log_{10}$ PFU mL^{-1}) = $\log_{10}C - \log_{10}S$, where C is the virus concentration in the control sample, and S is the virus concentration after the incubation with the SDS.

2.8. Biocompatibility in vitro

The potential cytotoxic activity and biological reactivity of the PP samples treated with a large plasma device and coated with 1 %, 0.25 %, or 0.1 % SDS were evaluated in vitro, according to the International Standard ISO 10993-5, Biological evaluation of medical devices - Part 5: Tests for in vitro cytotoxicity [42]. Samples were prepared in accordance with ISO 10993-12, Biological evaluation of medical devices - Part 12: Sample preparation and reference materials (ISO 10993-12) [47]. Five pieces of treated textile were cut into 3 cm^2 pieces and extracted in a complete growth medium (MEM supplemented with 10 % FBS, 4 mM L-glutamine, 0.11 mg mL^{-1} sodium-pyruvate, 100 IU mL^{-1} penicillin, and 100 μg mL^{-1} streptomycin) at a concentration of 3 cm^2 mL^{-1} with shaking for 24 ± 1 h at 37 °C, 5 % CO_2, for. A vehicle control (VC, complete cell culture medium incubated under extraction conditions), a negative control (NC, fresh complete cell culture medium), and a positive control (PC, 5 % DMSO) were included in the experiments. Three independent experiments with five replicates were performed. Graded concentrations (100 %, 50 %, and 25 %) of the extracts, prepared by dilution in VC, were tested. Sample controls (plasma-treated PP and receiving the same volume of MilliQ water, plasma-treated PP without any coating, and untreated polypropylene) were also included.

The mouse fibroblast cell line L-929 (NCTC clone 929 [L cell, L-929, derivative of Strain L] (ATCC® CCL-1™)) was used as the test system. Cells were seeded on 96-well plates at a density of 10000 cells/well and allowed to adhere overnight. The next day, the cell medium was replaced with graded concentrations of the sample extracts. Cytotoxicity was assessed after 24 ± 1 h of exposure using the 3 (4,5 dimethylthiazol-2-yl)-2,5 diphenyltetrazolium bromide (MTT) assay. Samples were considered cytotoxic if L929 cell viability was reduced by >30 % in the MTT test. Biological reactivity was evaluated by light microscopy (see Supporting Information Fig. S4) after 24 ± 1 and 48 ± 1 h of exposure and graded on a scale of 0 to 4 as described in ISO 10993-5. Samples were considered biologically reactive if they induced morphological changes that were rated higher than Grade 2, which is defined as up to 50 % of cells with morphological changes (roundness, devoid of intracytoplasmic granules, lysed) or up to 50 % reduction in cell growth. The GraphPad Prism 9 program (GraphPad Software, San Diego, CA, USA)

was used for statistical analysis (ANOVA and $P \leq 0.01$ was considered significant) data visualization.

2.9. Viral filtration efficiency and virus inactivation on masks

To evaluate if masks retain their filtration capabilities, VFE tests were performed in accordance with the EN 1483:2019 + AC 2019 (Medical face masks. Requirements and test methods) as previously described [48]. Briefly, three 10 cm × 10 cm pieces of PP were treated with the large plasma system, coated with 0.1 % SDS, and joined with a middle PET layer and an untreated outer PP layer to construct three-layer medical masks. VFE tests were performed on three masks with (treated mask) or without the functionalized layer (untreated mask) fixed in the VFE system and exposed to 13 μL of aerosolized phi6 virus-containing droplets, with the initial concentration of 7 $\log_{10}$ for 1 min, followed by 2 min of airflow. A positive control was performed before and after each set of three masks, in which no mask was fixed in the system. All filtration experiments were conducted by suction through the mask, which resulted in an airflow of 10 L min^{-1}. An impinger (SKC, Dorset, UK) containing 10 mL of peptone water was used to collect droplets that were not stopped by the mask, from which virus concentration was determined as described above. Furthermore, the procedure was expanded to also evaluate the number of surviving viruses on the material after the filtration assay. After the sample underwent the testing process, the layer made from plasma-treated PP incubated with SDS was removed from the device, placed in a 50 mL falcon tube, and incubated in the dark for 2 h. After incubation, 10 mL of SM buffer was poured into the falcon tube, vortexed, and used for subsequent viral quantification assay, as described in the section Infectivity assays.

2.10. Breathability

Breathability tests were performed at Lotrič Meroslovje d.o.o. company (Slovenia) in accordance with EN 14683:2019: Medical face masks – requirements and test methods standard [43]. Briefly, the constructed masks were fitted onto the test apparatus, which measures the differential pressure required to draw air through the filtering sample fixed on a holder with a diameter of 25 mm. The airflow was kept constant at 8 L min^{-1} in standard conditions. Three samples were tested per treatment, with five measurements per sample.

3. Results and discussion

3.1. Characterization of surface properties of plasma-treated non-woven polypropylene

The PP textiles were treated in either the small- or large-scale RF plasma reactor (see Experimental section), and the wettability was probed by measuring the water contact angle (WCA) within a minute after plasma treatment.

Fig. 4 shows the wettability improvement of non-woven PP after plasma treatment. When plasma was ignited at 0 sccm O_2 (1 Pa), a complete PP sample's wettability (i.e., immeasurably low WCA) was achieved already after 7 s of treatment time. The addition of small amounts (5 sccm) of oxygen to the plasma reactor enhanced treatment efficiency because an initial drop in the value of the contact angle appeared at a shorter treatment time. Namely, the WCA well below 10° was observed already after 3 s of plasma treatment, as shown in Fig. 4. However, complete wettability was obtained after a similar duration of treatment (i.e., 7 s). When the amount of oxygen added to the plasma reactor was increased to 30 sccm, it failed to reach the same effect. A large statistical error is observed for some measured points in Fig. 4, which was determined by calculating the standard deviation, considering several measurements on the same sample but at different locations. The error bars are particularly large for samples of moderate WCA (between 20 and 80°). The water droplet was absorbed in the textile at certain locations, but at others, it remained on the surface for a long time. The conclusion was that the ability of the plasma-treated PP samples to absorb the water droplet depends on small details, and it is not gradual. Since 10-s treatments provided beneficial WCA, this was the chosen treatment time for further experiments.

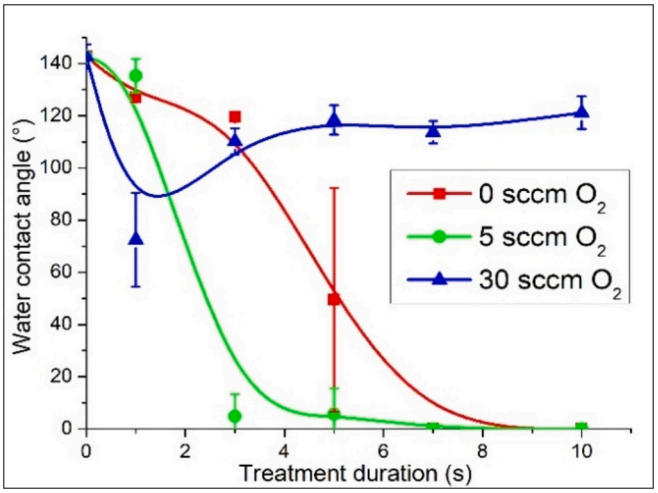

Fig. 4. Wettability of polypropylene textiles versus the treatment time. The water contact angle was measured within a minute after treatment in plasma sustained in the discharge chamber during the introduction of oxygen at different flow rates.

To disclose more information about the modified surface of plasma-treated PP, a comparison of high-resolution carbon C1s spectra of samples treated for 10 s is displayed in Fig. 5. As expected for PP, the untreated sample shows one symmetrical peak corresponding to C – C/C – H bonds. For plasma-treated samples, a typical tail is observed on the high binding energy side due to the formation of oxygen-functional groups during plasma treatment, as shown in Supplemental materials. A significant difference is observed when comparing plasma treatment at a base pressure (water vapor) or in oxygen – the subpeak at approximately 289 eV, which corresponds to O=C – O (carboxyl or ester groups), is more pronounced for O_2 plasma treatment for 10 s. This means that oxygen plasma treatment at a rather low flow rate leads to higher amounts of highly polar functional groups, such as O=C – O groups, on the surface of the PP textiles.

XPS results in Table 2 further corroborate these findings. The

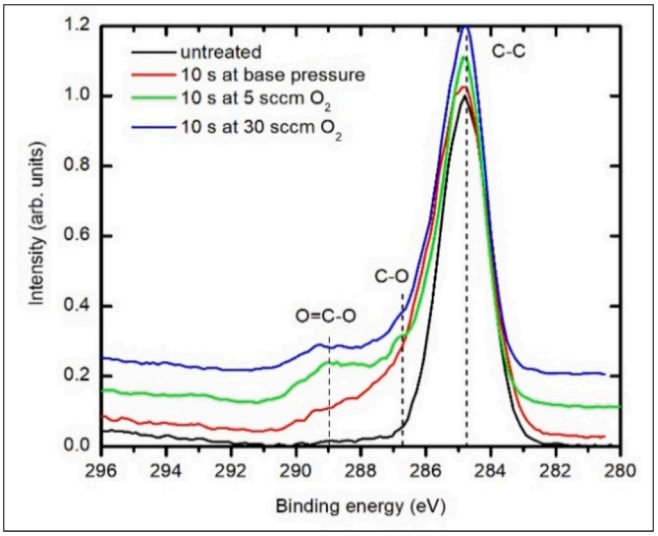

Fig. 5. Comparison of XPS C1s spectra of PP samples treated for 10 s.

Table 2
Percent of carbon and oxygen content of plasma-treated non-woven polypropylene material (XPS spectra fitting can be found under Supporting Information, Figs. S1, S2, and S3).

Sample	C	O	C – C	C – O	C=O	O=C – O
Untreated PP	95.9 ± 0.5	4.1 ± 0.5	100.0			
Base pressure, 7 s	84.5 ± 0.4	15.6 ± 0.4	77.7	14.8	5.0	2.5
Base pressure, 10 s	80.7 ± 0.3	19.4 ± 0.3	76.5	14.2	6.6	2.6
5 sccm O_2, 7 s	79.8 ± 0.6	20.2 ± 0.6	79.1	10.6	5.6	4.7
5 sccm O_2, 10 s	75.3 ± 0.9	24.7 ± 0.9	71.0	16.5	6.4	6.1
30 sccm O_2, 7 s	80.8 ± 0.5	19.2 ± 0.5	72.7	16.3	5.7	5.4
30 sccm O_2, 10 s	82.9 ± 0.7	17.1 ± 0.7	73.1	16.2	5.0	5.7

percentage of oxygen in the layer of the PP material, as probed by XPS, is lower for treatment at 0 sccm O_2 than in 5 sccm O_2 treatment, although the wettability of the sample treated at 0 sccm O_2 is as good as for the sample treated at 5 sccm O_2 for the same time (7 s). Furthermore, the oxygen concentration in the surface film of the PP fibers (as probed by XPS) treated at 30 sccm O_2 for 7 s is as large as for samples treated at lower gas flows. A detailed explanation of this paradox is beyond the scope of this article. However, a brief explanation is provided: The XPS is a surface-sensitive method for material characterization, so it detects only the composition on the surface of the fibers on the top of the textile-facing plasma. On the other hand, super-hydrophilicity (i.e., absorption of the water droplet inside the textile and thus immeasurably low WCA) is obtained only if the fibers inside the textiles are also functionalized with polar functional groups. The penetration of plasma radicals, which cause the functionalization of the polymer fibers inside porous materials such as textiles, depends on the diffusion, which depends on the pressure. If the pressure is increased, the diffusion is suppressed, so the penetration of radicals into the textile is poor. Primc et al. explained the penetration of radicals in textiles in detail [49]. The wettability is also improved by absorption of VUV radiation, which causes bond scission and, thus, oxidation of the polymer fibers' surface even in the absence of plasma radicals such as O atoms. The intensity of VUV radiation increases with decreasing pressure [50] because the electron temperature in non-equilibrium plasma increases with decreasing pressure. Finally, the exothermic surface reactions increase with increasing pressure. The density of reactive species that cause exothermic reactions increases with increasing pressure in the range of pressures up to about 100 Pa [51]. The polar surface functional groups are unstable but tend to reorient towards the bulk spontaneously at elevated temperatures [52]. The treatment of fibrous polymer material at elevated pressure causes increased temperature of fibers on the surface of the polypropylene textile, rapid re-orientation of the oxygen-containing functional groups, and thus the loss of the wettability despite the high concentration of oxygen in the surface film of the PP fibers as revealed from XPS spectra. The heating increases with increasing treatment time, which explains the rather unexpected minimum on the curve for 30 sccm oxygen flow in Fig. 4. In light of these arguments and obtained results, the materials used for antiviral studies were treated with oxygen plasma supplied at 5 sccm for 10 s to ensure complete wettability of treated samples before the application of appropriate SDS concentrations.

A detailed explanation of how plasma interacts with the surface of PP textiles, resulting in changes in surface chemical composition and physical structure, should take into account all reactive species that come in contact with the polymer surface. Plasma sustained at low pressure in oxygen or residual atmosphere (predominantly water vapor in hermetically tight systems) is a source of free electrons, positively and negatively charged ions, neutral radicals, and radiation. The exact mechanisms of interaction between oxygen or moist oxygen plasma with polyolefins is still a subject of scientific interest and recent results reveal complex surface reactions [53–55].

In our case, the samples are always at a floating potential, so the textile surface assumes a negative charge against the plasma potential. The surface negative charge prevents all negatively charged ions from reaching the textile. The electrons from the high-energy tail of the distribution function will reach the surface because their kinetic energy in plasma is higher than the potential drop across the sheath between the plasma and the sample surface. Still, the plasma electrons are retarded by the negative surface charge, so their kinetic energy when impinging the polymer surface is marginal. On the other hand, the negative surface charge will attract positively charged ions and they will be accelerated when passing the sheath. The mean free path between collisions at the pressure of 10 Pa is roughly 1 mm, and the sheath thickness in weakly ionized plasma is similar, so many ions will bombard the polymer surface with the kinetic energy that corresponds to the plasma-to-floating potential. The positively charged ions will cause bond scission and thus modify the surface properties of the polymer. Their penetration depth will be up to a few monolayers only, so their effect is limited to the very surface.

On the other hand, the radiation arising from plasma will penetrate deeper than the positively charged ions. Low-pressure plasma is an extensive source of radiation, and the radiation in the VUV range is usually predominant [56]. The VUV radiation will cause bond scission in the surface film and thus provide dangling bonds for neutral radicals. The latter do not feel the potential within the sheath, so they will impinge the surface with a marginal kinetic energy. They are, however, chemically reactive and interact with the polymer even in the absence of VUV radiation [57]. The OH radicals, which are formed in plasma in the residual atmosphere by dissociation of water vapor molecules, have a high oxidation potential and will interact extensively with the polyolefin surfaces by subtraction of hydrogen and thus formation of a dangling bond, which will be occupied by another OH radical of oxygen atom to form a polar functional group [58]. The combined effect of the positively charged ions, VUV radiation, and the radicals is the surface chemical composition, as shown in Table 2, and the wettability, as shown in Fig. 4.

3.2. *Virus inactivation on plasma-treated polypropylene textile*

Following plasma treatment, the PP samples underwent an impregnation procedure with different SDS solutions. The final concentration of SDS on the material is expressed in *w*/w % (e.g., 10 μg of SDS per 1 mg of PP is 1 % SDS). The results of virus inactivation assays are presented in Table 3. SDS interacts with the lipid envelope and viral proteins, which either disrupts the viral structure entirely or merely produces conformational changes of key structures to render the virus unable to infect its host (i.e., inactivated virus). Even 0.1 w/w % of SDS, applied to plasma pre-treated textiles, was able to effectively inactivate high concentrations of phi6, i.e., 6 $\log_{10}$ PFU mL^{-1}, following a 2-h incubation period. The inactivation efficiency lowered with the reduction in SDS concentration (0.05 %), resulting in inactivation of only 1.6 $\log_{10}$ PFU mL^{-1} of phi6.

Any materials may lose their functional properties upon storage because of irreversible reactions. In the case of plasma-pretreated textiles, the reactions may include the chemical interaction of plasma-

Table 3
Antiviral activity of various SDS concentrations (*w*/w %), applied to polypropylene treated with plasma for 10 s.

Sample ($n = 3$)	Virus conc. ($\log_{10}$ PFU mL^{-1})
Control	6.72 ± 0.02
Plasma pre-treated PP	6.70 ± 0.39
1 % SDS	0[a]
0.25 % SDS	0[a]
0.1 % SDS	0[a]
0.05 % SDS	5.11 ± 0.11

[a] When no plaques were present, the viral concentration is presented as 0;

modified polymer surfaces with adsorbed reagents. In order to determine the treatment durability of functionalized PP, i.e., whether it retains its antiviral activity in time, we stored samples in the dark at ambient conditions and tested their antiviral activity every few days/weeks, with the first test performed 7 days after deposition of the antiviral agent. Altogether, 7 measurements were done, and, in all cases, no plaques were observed, except at the last point of testing (125th day), where some plaques were present on plates with the lowest SDS concentration (Fig. 6). Nevertheless, inactivation for over 6 orders of magnitude was determined at all tested SDS concentrations, which is an excellent antiviral performance.

Some PP samples were also incubated with viruses for times shorter than 2 h. Fig. 7 shows the inactivation rate of phi6 virus exposed to PP with 0.1 % SDS. The initial virus concentration (approx. 10^8 PFU mL^{-1}) is in the upper range of what a natural exposure to a virus would be [59]. Incubation for 30 min causes the decrease of the infective viruses by about 4 orders of magnitude, while after an hour, the concentration of infective viruses fell below the detection limit. This experiment confirms that antiviral activity is rapid and effective for the studied virus. The results are highly reproducible since the error bars are marginal for all measured values in Fig. 7.

The wettability after plasma treatment of PP and after applying different SDS solutions was also studied. After applying 0.05, 0.1, 0.25, and 1 % SDS solutions to plasma-treated PP, the samples were dried at ambient conditions (25 °C, 50 % relative humidity); thereafter water droplets were re-applied. It was found that the surface remained superhydrophilic, i.e., it immediately absorbed a water droplet. Therefore, we measured water droplets' absorption times, which are shown in Table 4.

The SDS concentration influences the speed of absorption, which can be explained by its surfactant properties. The higher the SDS concentration, the more pronounced the ability of SDS-applied PP to stretch a droplet.

3.3. Biocompatibility in vitro

The biocompatibility (cytotoxicity and biological reactivity) of the PP samples treated with 1 %, 0.25 % and 0.1 % SDS was evaluated in vitro in the L929 mouse fibroblast cell line, according to ISO 10993-5 [42], which describes test methods to assess the in vitro cytotoxicity of medical devices and is used in the evaluation process of medical devices, including face masks and materials intended for the production of face masks. The results of the cytotoxicity testing (Fig. 8) showed that the sample with 1 % SDS was cytotoxic for L929 cells, reducing cell viability by >30 %, whereas a lower concentration of SDS did not induce

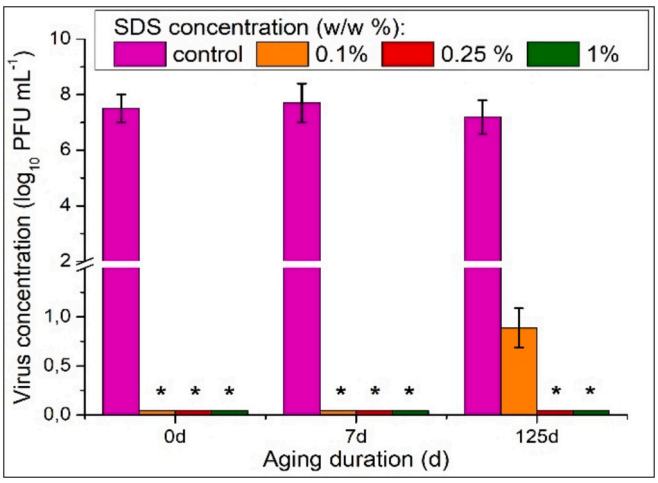

Fig. 6. Antiviral activity of SDS-impregnated polypropylene stored at room temperature for up to 125 days. The "*" marks samples where no infectious viral particles were recovered.

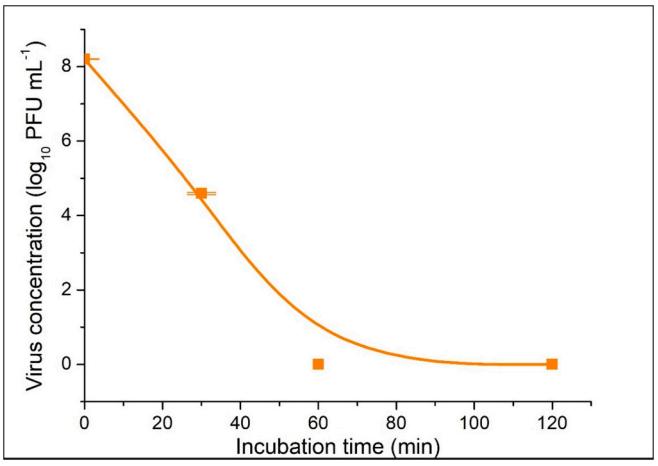

Fig. 7. Time-dependent inactivation of phi6 on 0.1 % SDS-covered PP. The standard deviation bars are too small to be visible at this scale.

Table 4
Water droplets absorption times after applying them on the already SDS-conditioned and three hours dried PP.

SDS conc (%)	Absorption time (s)	stdev
1	0.054	0.015
0.25	0.116	0.04
0.1	0.257	0.03

cytotoxicity. None of the tested sample controls (plasma-treated PP and receiving the same volume of MilliQ water, plasma-treated PP without any coating, and untreated PP) were cytotoxic for L929 cells.

SDS is known to cause eye and skin irritation and may cause respiratory irritation. However, it is commonly used in cosmetics and cleaning products and even added to food in low concentrations [36]. A cytotoxic SDS concentration of around 100 μg mL^{-1} was recently reported for L929 cells [60]. Assuming a complete SDS elution from 3-cm^2 samples into the growth media, the final SDS concentrations of 1 %, 0.25 %, and 0.1 % samples would be 153 μg mL^{-1}, 38.25 μg mL^{-1}, and 15.3 μg mL^{-1}, respectively. Thus, the 50 % and 25 % SDS dilutions of 1 % material would contain 76.3 μg mL^{-1} and 38.25 μg mL^{-1}, respectively. This coincides with the results reported by [60], where SDS concentrations between 80 and 100 μg mL^{-1} resulted in minor cytotoxicity towards cells, and below 60 μg mL^{-1}, no adverse effects were observed. Our results also indicated this, as none of those samples were cytotoxic. Therefore, by reducing the concentration of SDS in the PP samples (samples with 0.25 % and 0.1 % SDS) also, the cytotoxicity of the sample extract was reduced entirely, leaving no effect on cell viability after exposure to either non-diluted or diluted sample extracts (100, 50 or 25 %). Additionally, a 10 × 10 cm mask treated with 0.1 % SDS solution would contain approximately 51 μg of SDS, far below where adverse effects would be expected.

Cell morphology was evaluated and graded on a scale from 0 (no changes in morphology) to 4 (severe changes in morphology), according to ISO 10993-5 standard (Fig. 9) [42]; scanning electron micrographs are available in Supplemental materials. The NC and VC samples showed no morphological changes and were rated Grade 0 at both time points. The PC sample caused growth reduction and cell lysis and was rated Grade 3 after 24 h and Grade 4 after 48 h of exposure. The non-diluted PP sample with 1 % SDS showed severe biological reactivity (Grade 4) at both exposure times; the twice diluted extract was rated with mild (Grade 2) after 24 h and moderate reactivity (Grade 3) after 48 h, while the four-times diluted sample extract showed slight (Grade 1) reduction after both exposure times. None of the sample controls showed more than slight biological reactivity (Grades 0–1), confirming SDS to be the

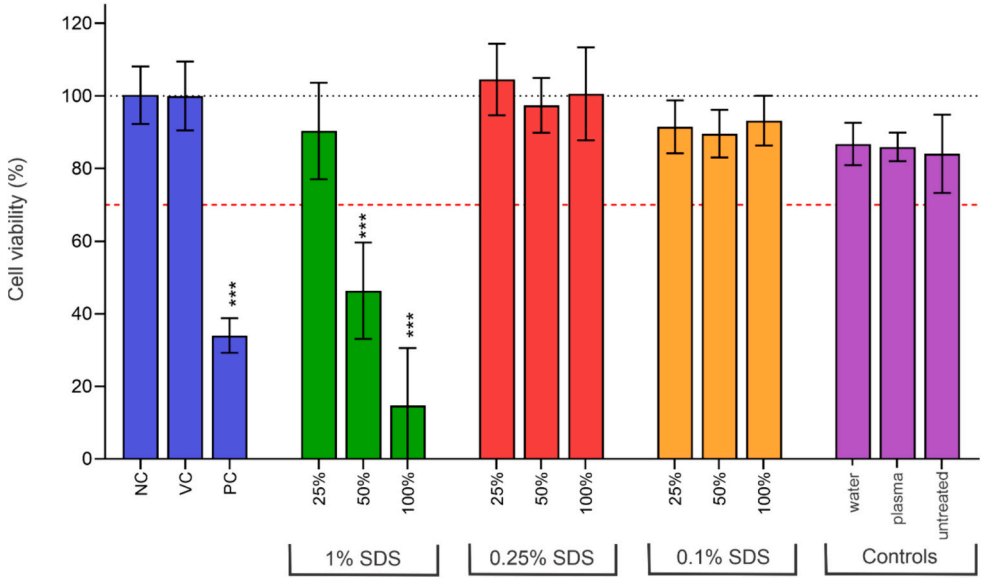

Fig. 8. Cytotoxicity of polypropylene with different SDS concentrations. Changes in cell viability after 24 h of exposure of L929 cells to graded concentrations of samples with 1, 0.25, and 0.1 % SDS are shown. Data are presented as a percentage of the vehicle control (VC, complete cell culture medium incubated under extraction conditions). NC is the negative control (fresh complete cell culture medium), and PC is the positive control (5 % DMSO). Only the highest tested extract concentration, which was 100 % of the sample controls (water, plasma, and untreated polypropylene), is shown. The dotted line represents the viability of cells in the VC sample. The red dotted line represents the cytotoxicity threshold value of 70 % viability. The asterisks denote statistically significant differences from the negative control (ANOVA and Dunnet's multiple comparison test; ***$p < 0.001$). (For interpretation of the references to colour in this figure legend, the reader is referred to the web version of this article.)

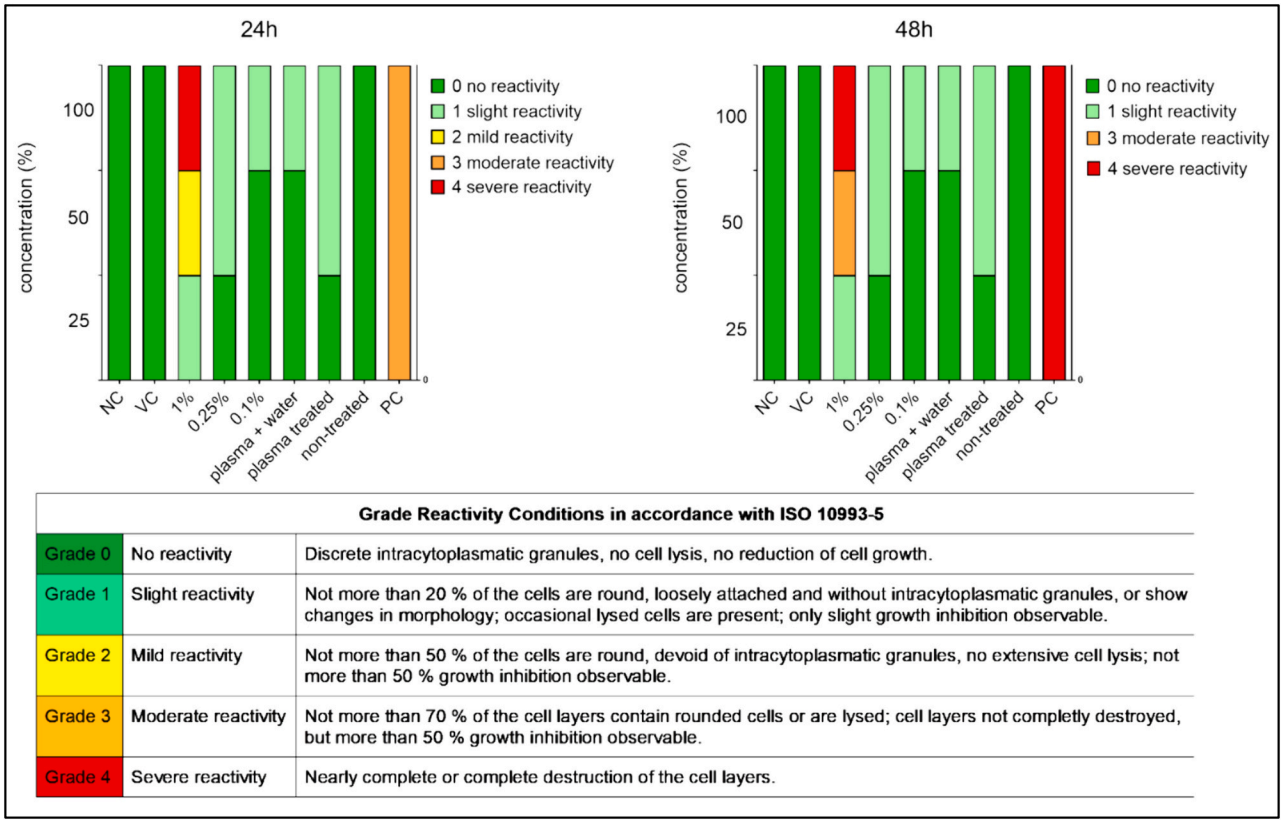

Grade Reactivity Conditions in accordance with ISO 10993-5		
Grade 0	No reactivity	Discrete intracytoplasmatic granules, no cell lysis, no reduction of cell growth.
Grade 1	Slight reactivity	Not more than 20 % of the cells are round, loosely attached and without intracytoplasmatic granules, or show changes in morphology; occasional lysed cells are present; only slight growth inhibition observable.
Grade 2	Mild reactivity	Not more than 50 % of the cells are round, devoid of intracytoplasmatic granules, no extensive cell lysis; not more than 50 % growth inhibition observable.
Grade 3	Moderate reactivity	Not more than 70 % of the cell layers contain rounded cells or are lysed; cell layers not completly destroyed, but more than 50 % growth inhibition observable.
Grade 4	Severe reactivity	Nearly complete or complete destruction of the cell layers.

Fig. 9. Biological reactivity of the PP sample extracts with different % of SDS after 24 and 48 h of exposure in the L929 mouse fibroblast cell line. Morphological changes were evaluated and graded according to ISO 10993-5. NC is the negative control (fresh cell culture medium), and VC is the vehicle control (complete cell culture medium incubated under extraction conditions). PC is the positive control (5 % DMSO). The assay controls were tested at only one concentration, and a uniform bar is shown for visualization.

causative agent in the observed biological reactivity. Further on, the PP samples with lower SDS concentrations, e.g., 0.25 % and 0.1 %, were also rated Grade 0–1 at both exposure times, which is, according to ISO 10993-5, not considered as biological reactivity. As both the cytotoxicity and biological reactivity test confirmed the in vitro biocompatibility of the PP samples with lower SDS concentration, and already the sample with 0.1 % SDS showed strong antiviral activity, this sample was used as material for the preparation of face masks, which were further tested for virus filtration efficiency, virus inactivation on masks, and breathability.

3.4. Viral filtration efficiency, virus inactivation on masks, and breathability

According to EN 14683:2019: Medical face masks – requirements and test methods standard, the bacterial filtration efficiency of Type II medical masks should be above 98 % and have a breathability value no higher than 40 Pa cm^{-2}. Therefore, the virus filtration efficiency (VFE) of the mask should also achieve a value of at least 98 %. The summarized results (Table 5) show that the masks prepared with treated PP textiles satisfy these parameters and display no detrimental differences compared to the untreated masks. The important distinction is that the phi6 virus remains infective on the surfaces of untreated masks, while no infectious virus was recovered from the masks prepared with the treated textile. This study's results support further development and application of masks and other PPE with antiviral or, broadly, antimicrobial activity.

4. Conclusion

The wettability of medical-grade polypropylene textiles was rapidly and sufficiently improved by treatment with a low-pressure gaseous plasma sustained by inductively coupled radio frequency discharge. The working gases were either water vapor (present in the vacuum system at the ultimate pressure of about 1 Pa) or oxygen. The best results were observed when treating PP textiles with oxygen plasma at an oxygen flow of 5 sccm for 10 s. Adding oxygen into gaseous plasma provides more reactants, predominantly neutral oxygen atoms in the ground state. Treatment at larger pressures did not provide satisfactory results despite rapid surface oxidation, as proved by XPS, which was explained by the peculiarities of our samples. The PP textile treated at appropriate discharge parameters enabled complete absorption of a severely diluted surfactant solution, which displays antimicrobial properties. At the 0.1 *w*/w % SDS concentration, the PP showed high virus inactivation of >7 log_{10} PFU mL^{-1} (concentration greater than usual naturally occurring exposures), which lasted for at least 125 days. Furthermore, PP with 0.1 % SDS had no cytotoxic effect or biological reactivity in the in vitro biocompatibility test, indicating the safety of textiles treated at appropriate parameters. Furthermore, the underlying properties of the treated material remained unchanged (e.g., VFE and breathability), adhering to EN 14683:2019: medical face masks – requirements and test standard, while the mask exhibited antiviral properties. The results reported in this article are promising for developing functional masks and filtering materials that not only capture infectious particles but also inactivate them, thus preventing infections spread by fomites and giving us an additional level of protection against current and future airborne disease outbreaks.

CRediT authorship contribution statement

Mark Zver: Writing – review & editing, Writing – original draft, Validation, Methodology, Investigation, Data curation. **David Dobnik:** Writing – review & editing, Supervision, Formal analysis. **Rok Zaplotnik:** Writing – review & editing, Writing – original draft, Visualization, Validation, Methodology, Investigation, Formal analysis, Data curation. **Miran Mozetič:** Writing – review & editing, Writing – original draft, Validation, Supervision, Funding acquisition, Conceptualization. **Alenka Vesel:** Writing – review & editing, Validation, Methodology, Investigation, Formal analysis, Data curation. **Arijana Filipić:** Writing – review & editing, Validation, Supervision, Methodology, Formal analysis. **Polona Kogovšek:** Writing – review & editing, Validation, Supervision, Conceptualization. **Katja Fric:** Validation, Investigation, Formal analysis. **Alja Štern:** Writing – review & editing, Validation, Supervision, Methodology, Investigation, Formal analysis. **Gregor Primc:** Writing – review & editing, Writing – original draft, Visualization, Supervision, Project administration, Methodology, Funding acquisition, Formal analysis, Conceptualization.

Table 5
Viral filtration efficiency, virus survival on treated masks, and breathability.

Sample ($n = 3$)	VFE (%)	Breathability (Pa cm^{-2})	Virus concentration (log_{10} PFU mL^{-1})
EN 14683:2019	≥98	<40	N/A
untreated masks	99.86 ± 0.11	31.26 ± 0.91	3.61 ± 0.48
0.1 % SDS mask	99.81 ± 0.32	31.56 ± 1.99	0[a]

[a] When no plaques were present, the viral concentration is presented as 0;

Declaration of competing interest

The authors declare the following financial interests/personal relationships which may be considered as potential competing interests: Mark Zver, David Dobnik, Rok Zaplotnik, Miran Mozetic, Alenka Vesel, Arijana Filipic, Polona Kogovsek, Katja Fric, Alja Stern reports financial support was provided by Public Research Agency of the Republic of Slovenia. Gregor Primc reports financial support was provided by Public Research Agency of the Republic of Slovenia. Miran Mozetic, Mark Zver, Rok Zaplotnik, Alenka Vesel, Arijana Filipic, David Dobnik, Polona Kogovsek, Maja Ravnikar has patent A method for preparation of virucidal polymer textile materials and virucidal face masks made from said materials pending to Jozef Stefan Institute, National Institute of Biology. Gregor Primc has patent A method for preparation of virucidal polymer textile materials and virucidal face masks made from said materials pending to Jozef Stefan Institute, National Institute of Biology. If there are other authors, they declare that they have no known competing financial interests or personal relationships that could have appeared to influence the work reported in this paper.

Data availability

Data will be made available on request.

Acknowledgments

The authors acknowledge the financial support of the Slovenian Research and Innovation Agency under core research funds P2-0082 (Thin-film structures and plasma surface engineering), P1-0245 (Ecotoxicology, toxicogenomics, and carcinogenesis), and P4-0407 (Environmental and applied virology: viruses, friends and foes, and project), L2-2617 (Innovative method for water purification). The authors would also like to thank the company Lotrič d.o.o. for carrying out breathability tests on finalized masks and the company Omega Air d.o.o. for providing the textile samples.

Appendix A. Supplementary data

Supplementary data to this article can be found online at https://doi.org/10.1016/j.porgcoat.2024.108827.

References

[1] J. Howard, A. Huang, Z. Li, Z. Tufekci, V. Zdimal, H.M. van der Westhuizen, et al., An evidence review of face masks against COVID-19, Proc. Natl. Acad. Sci. USA 118 (4) (2021) 1–12.

[2] A.W.H. Chin, J.T.S. Chu, M.R.A. Perera, K.P.Y. Hui, H.L. Yen, M.C.W. Chan, et al., Stability of SARS-CoV-2 in different environmental conditions, Lancet Microbe [Internet] 1 (1) (2020) e10. Available from: https://doi.org/10.1016/S2666-5247(20)30003-3.

[3] D.S. Morais, R.M. Guedes, M.A. Lopes, Antimicrobial approaches for textiles: from research to market, Materials 9 (6) (2016) 1–21.

[4] G. Sun, Antimicrobial textiles, in: Antimicrobial Textiles [Internet]. Gang Sun, Elsevier, 2016, pp. 1–337. Available from: https://linkinghub.elsevier.com/retrieve/pii/B9780081005767000018.

[5] S.M. Imani, L. Ladouceur, T. Marshall, R. Maclachlan, L. Soleymani, T.F. Didar, Antimicrobial nanomaterials and coatings: current mechanisms and future perspectives to control the spread of viruses including SARS-CoV-2, ACS Nano 14 (10) (2020) 12341–12369.

[6] B. Song, E. Zhang, X. Han, H. Zhu, Y. Shi, Z. Cao, Engineering and application perspectives on designing an antimicrobial surface, ACS Appl. Mater. Interfaces 12 (19) (2020) 21330–21341.

[7] C. Ma, A. Nikiforov, N. De Geyter, R. Morent, K. (Ken) Ostrikov, Plasma for biomedical decontamination: from plasma-engineered to plasma-active antimicrobial surfaces, Curr. Opin. Chem. Eng. [Internet] 36 (December 2021) (2022) 100764. Available from: https://doi.org/10.1016/j.coche.2021.100764.

[8] K. Verhaelen, M. Bouwknegt, S. Rutjes, A.M. de Roda Husman, E. Duizer, Wipes coated with a singlet-oxygen-producing photosensitizer are effective against human influenza virus but not against norovirus, Appl. Environ. Microbiol. 80 (14) (2014) 4391–4397.

[9] J. Lei, L. Yang, Y. Zhan, Y. Wang, T. Ye, Y. Li, et al., Plasma treated polyethylene terephthalate/polypropylene films assembled with chitosan and various preservatives for antimicrobial food packaging, Colloids Surf. B: Biointerfaces (114) (2014 Feb 1) 60–66.

[10] O. Plohl, V. Kokol, A. Filipić, K. Fric, P. Kogovšek, Z.P. Fratnik, et al., Screen-printing of chitosan and cationised cellulose nanofibril coatings for integration into functional face masks with potential antiviral activity, Int. J. Biol. Macromol. (2023 May 1) 236.

[11] Calais GB, Rocha Neto JBM, Bataglioli RA, Chevalier P, Tsukamoto J, Arns CW, et al. Bioactive textile coatings for improved viral protection: a study of polypropylene masks coated with copper salt and organic antimicrobial agents. Appl. Surf. Sci. [Internet] 2023 Nov;638:158112. Available from: https://linkinghub.elsevier.com/retrieve/pii/S0169433223017919.

[12] M.R. Badrossamay, G. Sun, Acyclic halamine polypropylene polymer: effect of monomer structure on grafting efficiency, stability and biocidal activities, React. Funct. Polym. 68 (12) (2008) 1636–1645.

[13] S. Ghosh, R. Mukherjee, D. Basak, J. Haldar, One-step curable, covalently immobilized coating for clinically relevant surfaces that can kill bacteria, fungi, and influenza virus, ACS Appl. Mater. Interfaces 12 (25) (2020 Jun 24) 27853–27865.

[14] J. Vartiainen, M. Rättö, S. Paulussen, Antimicrobial activity of glucose oxidase-immobilized plasma-activated polypropylene films, Packag. Technol. Sci. 18 (5) (2005 Sep) 243–251.

[15] D.J. da Silva, M.M. de Oliveira, S.H. Wang, D.J. Carastan, D.S. Rosa, Designing antimicrobial polypropylene films with grape pomace extract for food packaging, Food Packag. Shelf Life (2022 Dec 1) 34.

[16] S. Kim, J. Chung, S.H. Lee, J.H. Yoon, D.H. Kweon, W.J. Chung, Tannic acid-functionalized HEPA filter materials for influenza virus capture, Sci. Rep. 11 (1) (2021) 1–7. Available from: https://doi.org/10.1038/s41598-020-78929-4.

[17] M.H. Chua, W. Cheng, S.S. Goh, J. Kong, B. Li, J.Y.C. Lim, et al., Face masks in the new COVID-19 normal: materials, testing, and perspectives, Research 2020 (2020) 1–40.

[18] F. Zabihi, J. Reissner, A. Friese, M. Schulze, C. Nie, P. Nickl, et al., Development of functional filter materials for virus protective face masks, Adv. Mater. Technol. 8 (17) (2023 Sep 11).

[19] Q. Liu, Y. Zhang, W. Liu, L.H. Wang, Y.W. Choi, M. Fulton, et al., A broad-spectrum antimicrobial and antiviral membrane inactivates SARS-CoV-2 in minutes, Adv. Funct. Mater. 31 (47) (2021 Nov 1).

[20] E. Horváth, L. Rossi, C. Mercier, C. Lehmann, A. Sienkiewicz, L. Forró, Photocatalytic nanowires-based air filter: towards reusable protective masks, Adv. Funct. Mater. 30 (40) (2020 Oct 1).

[21] Y. Wang, R. Cao, C. Wang, X. Song, R. Wang, J. Liu, et al., In situ embedding hydrogen-bonded organic frameworks nanocrystals in electrospinning nanofibers for ultrastable broad-spectrum antibacterial activity, Adv. Funct. Mater. 33 (20) (2023 May 12).

[22] A. Cano-Vicent, A. Tuñón-Molina, M. Martí, Y. Muramoto, T. Noda, K. Takayama, et al., Antiviral face mask functionalized with solidified hand soap: low-cost infection prevention clothing against enveloped viruses such as SARS-CoV-2, ACS Omega 6 (36) (2021 Sep 14) 23495–23503.

[23] K. Takayama, A. Tuñón-Molina, A. Cano-Vicent, Y. Muramoto, T. Noda, J. L. Aparicio-Collado, et al., Non-woven infection prevention fabrics coated with biobased cranberry extracts inactivate enveloped viruses such as SARS-CoV-2 and multidrug-resistant bacteria, Int. J. Mol. Sci. 22 (23) (2021 Dec 1).

[24] M. Maton, S. Gabut, C. Neut, P. Odou, C. Sacareau, A. Pinon, et al., Antiviral functionalization of a polypropylene nonwoven textile structure as a self-decontaminating layer for respiratory masks, Biomater. Sci. 11 (10) (2023) 3502–3511.

[25] C. Arcona, K. Breder, D.K. Everts, C.J. Gasdaska, V. Hays, M.W. Klett, et al., Abrasives, in: Ullmann's Encyclopedia of Industrial Chemistry [Internet], John Wiley & Sons, Ltd, 2022, pp. 1–27. Available from: https://doi.org/10.1002/14356007.a01_001.pub2.

[26] T. Stegmaier, M. Linke, A. Dinkelmann, V. Von Arnim, H. Planck, Environmentally friendly plasma technologies for textiles, in: Sustainable Textiles: Life Cycle and Environmental Impact, Elsevier Inc., 2009, pp. 155–178.

[27] C. Ma, A. Nikiforov, N. De Geyter, X. Dai, R. Morent, K. Ostrikov, (Ken)., Future antiviral polymers by plasma processing, Prog. Polym. Sci. [Internet] 118 (2021) 101410. Available from: https://doi.org/10.1016/j.progpolymsci.2021.101410.

[28] N. Dehbashi Nia, S.W. Lee, S. Bae, T.H. Kim, Y. Hwang, Surface modification of polypropylene non-woven filter by O2 plasma/acrylic acid enhancing Prussian blue immobilization for aqueous cesium adsorption, Appl. Surf. Sci. (2022 Jul 15) 590.

[29] N.T. Xuan Nguyen, P. Daniel, J.F. Pilard, R. Cariou, F. Gigout, F. Leroi, Antibacterial activity of plasma-treated polypropylene membrane functionalized with living Carnobacterium divergens in cold-smoked salmon, Food Control (2022 Jul 1) 137.

[30] Z. Honarvar, M. Farhoodi, M.R. Khani, A. Mohammadi, B. Shokri, R. Ferdowsi, et al., Application of cold plasma to develop carboxymethyl cellulose-coated polypropylene films containing essential oil, Carbohydr. Polym. (176) (2017 Nov 15) 1–10.

[31] Labay C, Canal JM, Modic M, Cvelbar U, Quiles M, Armengol M, et al. Antibiotic-loaded polypropylene surgical meshes with suitable biological behaviour by plasma functionalization and polymerization. Biomaterials [Internet] 2015;71:132–44. Available from: https://doi.org/10.1016/j.biomaterials.2015.08.023.

[32] A. Haji, M. Khajeh Mehrizi, M. Sarani, Surface modification of polypropylene nonwoven by plasma and β-Cyclodextrin: optimization and cationic dye removal studies, Surf. Interfaces (2021 Aug 1) 25.

[33] M. Gryta, Surface modification of polypropylene membrane by helium plasma treatment for membrane distillation, J. Membr. Sci. (2021 Jun 15) 628.

[34] X.C. He, H.Y. Yu, Z.Q. Tang, L.Q. Liu, M.G. Yan, J.S. Gu, et al., Reducing protein fouling of a polypropylene microporous membrane by CO2 plasma surface modification, Desalination 244 (1–3) (2009 Aug) 80–89.

[35] C. Zhang, J. Jin, J. Zhao, W. Jiang, J. Yin, Functionalized polypropylene non-woven fabric membrane with bovine serum albumin and its hemocompatibility enhancement, Colloids Surf. B: Biointerfaces (102) (2013 Feb 1) 45–52.

[36] M.M. Singer, R.S. Tjeerdema, Fate and Effects of the Surfactant Sodium Dodecyl Sulfate, 1993.

[37] M. Simon, M. Veit, K. Osterrieder, M. Gradzielski, Surfactants – compounds for inactivation of SARS-CoV-2 and other enveloped viruses, Curr. Opin. Colloid Interface Sci. [Internet] 55 (2021) 101479. Available from: https://doi.org/10.1016/j.cocis.2021.101479.

[38] M.K. Howett, E.B. Neely, N.D. Christensen, B. Wigdahl, F.C. Krebs, D. Malamud, et al., A Broad-spectrum Microbicide With Virucidal Activity against Sexually Transmitted Viruses [Internet] 43 (1999). Available from: https://journals.asm.org/journal/aac.

[39] A. Kumar, W.A. Ansari, T. Ahamad, M. Saquib, M.F. Khan, Safe use of sodium dodecyl sulfate (SDS) to deactivate SARS-CoV-2: an evidence-based systematic review, Coronaviruses 2 (9) (2021) 1–6.

[40] International Organization for Standardization. ISO 18184:2019 Textiles Determination of Antiviral Activity of Textile Products [Internet]. 2019 [cited 2023 Oct 20]. Available from: https://www.iso.org/standard/71292.html.

[41] N. Turgeon, M.J. Toulouse, B. Martel, S. Moineau, C. Duchaine, Comparison of five bacteriophages as models for viral aerosol studies, Appl. Environ. Microbiol. 80 (14) (2014) 4242–4250.

[42] International Organization for Standardization. ISO 10993-5:2009 Biological Evaluation of Medical Devices Part 5: Tests for In Vitro Cytotoxicity [Internet]. 2009 [cited 2023 Oct 20]. Available from: https://www.iso.org/standard/36406.html.

[43] European Standards. BS EN 14683:2019 Medical Face Masks. Requirements and Test Methods [Internet]. 2019 [cited 2023 Oct 20]. Available from: https://www.edana.org/docs/default-source/international-standards/nbn-en-14683_2019-ac-2019_e.pdf?sfvrsn=3797c92b_4.

[44] M. Mozetič, A. Vesel, G. Primc, R. Zaplotnik, Introduction to plasma and plasma diagnostics. Non-thermal plasma technology for polymeric materials: applications in composites, Nanostructured Materials, and Biomedical Fields (2019 Jan 1) 23–65.

[45] R. Zaplotnik, A. Vesel, M. Mozetic, A fiber optic catalytic sensor for neutral atom measurements in oxygen plasma, Sensors 12 (4) (2012 Apr) 3857–3867.

[46] N.K. Beck, K. Callahan, S.P. Nappier, H. Kim, M.D. Sobsey, J.S. Meschke, Development of a spot-titer culture assay for quantifying bacteria and viral indicators, J. Rapid Methods Autom. Microbiol. 17 (4) (2009) 455–464.

[47] International Organization for Standardization, ISO 10993-12 biological evaluation of medical devices - part 12: sample preparation and reference materials, BSI British Standards1, 2004, pp. 1–20.

[48] A. Filipić, K. Fric, M. Ravnikar, P. Kogovšek, Assessment of different experimental setups to determine viral filtration efficiency of face masks, Int. J. Environ. Res. Public Health 19 (22) (2022 Nov 1).

[49] Primc G, Zaplotnik R, Vesel A, Mozetič M. Mechanisms involved in the modification of textiles by non-equilibrium plasma treatment. Vol. 27, Molecules. MDPI; 2022.

[50] Popović D, Mozetič M, Vesel A, Primc G, Zaplotnik R. Review on vacuum ultraviolet generation in low-pressure plasmas. Plasma Process. Polym. [Internet] 2021 Sep 18;18(9):2100061. Available from: https://doi.org/10.1002/ppap.202100061.

[51] Primc G. Generation of neutral chemically reactive species in low-pressure plasma. Front. Phys. [Internet] 2022 May 12;10. Available from: https://doi.org/10.3389/fphy.2022.895264/full.
[52] J.H. Oh, M.W. Moon, C.H. Park, Effect of crystallinity on the recovery rate of superhydrophobicity in plasma-nanostructured polymers, RSC Adv. 10 (18) (2020 Mar 16) 10939–10948.
[53] R.C. Longo, A. Ranjan, P.L.G. Ventzek, Density functional theory study of oxygen adsorption on polymer surfaces for atomic-layer etching: implications for semiconductor device fabrication, ACS Appl. Nano Mater. 3 (6) (2020 Jun 26) 5189–5202.
[54] J. Polito, M. Denning, R. Stewart, D. Frost, M.J. Kushner, Atmospheric pressure plasma functionalization of polystyrene, J. Vac. Sci. Technol. A 40 (4) (2022 Jul 1).
[55] V.S.S.K. Kondeti, Y. Zheng, P. Luan, G.S. Oehrlein, P.J. Bruggeman, O·, H·, and ·OH radical etching probability of polystyrene obtained for a radio frequency driven atmospheric pressure plasma jet, J. Vac. Sci. Technol. A 38 (3) (2020 May 1).
[56] D. Popović, M. Mozetič, A. Vesel, G. Primc, R. Zaplotnik, Review on vacuum ultraviolet generation in low-pressure plasmas, Plasma Process. Polym. [Internet] 18 (9) (2021 Sep 18), https://doi.org/10.1002/ppap.202100061. Available from:.
[57] A. Vesel, R. Zaplotnik, M. Mozetič, G. Primc, Surface modification of PS polymer by oxygen-atom treatment from remote plasma: initial kinetics of functional groups formation, Appl. Surf. Sci. (2021 Sep 30) 561.
[58] A. Vesel, R. Zaplotnik, G. Primc, M. Mozetič, Evolution of surface functional groups and aromatic ring degradation upon treatment of polystyrene with hydroxyl radicals, Polym. Degrad. Stab. (2023 Dec 1) 218.
[59] J. Li, Z. Cheng, Y. Zhang, N. Mao, S. Guo, Q. Wang, et al., Evaluation of infection risk for SARS-CoV-2 transmission on university campuses, Sci. Technol. Built Environ. 27 (9) (2021) 1165–1180.
[60] Y.J. Lee, Y.J. Ahn, G.J. Lee, Cytotoxicity evaluation of sodium lauryl sulfate in a paper-based 3D cell culture system, Anal. Methods 14 (18) (2022) 1755–1764.